

SURROGATE SYNTHESIS OF FRAME EDDY CURRENT PROBES WITH UNIFORM SENSITIVITY IN THE TESTING ZONE

Volodymyr Ya. Halchenko, Ruslana Trembovetska, Volodymyr Tychkov

Cherkasy State Technological University, Instrumentation, Mechatronics and Computer Technologies Department, Blyd. Shevchenka, 460, 18006, Cherkasy, Ukraine, (✉ halchvl@gmail.com, r.trembovetska@chdtu.edu.ua, v.tychkov@chdtu.edu.ua, +380 972 614 836)

Abstract

A mathematical method for nonlinear surrogate synthesis of frame surface eddy current probes providing a uniform eddy current density distribution in the testing object area is proposed. A metamodel of a frame movable eddy-current probe with a planar excitation system structure, used in the algorithm for surrogate optimal synthesis was created. The examples of a nonlinear synthesis of excitation systems with the application of the modern metaheuristic stochastic algorithms for finding the global extremum are considered. The numerical findings of the problem analyses are presented. The efficiency of the synthesized excitation structures was demonstrated on the basis of the eddy current density distribution graphs on the surface of the control zone of the object in comparison with classical analogues.

Keywords: eddy current probe, uniform sensitivity, metamodel, additive neural network regression, surrogate optimization, global extremum.

© 2021 Polish Academy of Sciences. All rights reserved

1. Introduction

The use of eddy current testing means with excitation sources, providing an optimal *electromagnetic field* (EMF) to create a uniform sensitivity to the defect detection in the *testing object* (TO) volume and to determine their geometric parameters in an automated mode contributes to the successful solution of flaw measurement problems.

A number of authors have proposed the creation of a uniform, initially given tangential EMF of excitation [1–6] in order to improve the selectivity and ensure the uniform sensitivity of *surface eddy current probes* (SECPs). *Excitation systems* (ESs), generating uniform configurations of EMFs in the testing zone are discussed in those works. As a rule, they refer to the excitation of uniform *eddy current density* (ECD) distribution in a stationary TO. Only some works, for example [7–9], deal with the homogeneous configuration of ECD on the TO surface merely for the stationary SECPs. The review article [10] thoroughly analyses modern scientific research on the creation of SECPs with various ESs, providing optimal excitation EMFs in the testing zone.

Based on this analysis, it should be noted that a significant number of studies aimed only at creating an EMF with predetermined properties for a stationary SECP, while a similar problem of creating movable probes has not been studied. However, the widespread use of automated testing processes with the application of the eddy current method requires considering the effect of speed and changes in ECD distribution caused by the action of transfer currents. Therefore, the design of a moving SECP with an ES which provides an initially given uniform distribution of ECD in the TO, proves to be topical. The efforts of the authors are directed specifically at solving the problem of creating movable SECP with different structures of the ES, ensuring a uniform ECD distribution. Thus, the published work [11] presents the results of the first attempts at optimal surrogate synthesis of a movable circular SECP. At the same time, it is necessary to study SECPs with frame ES structures in the sense of considering the possibility of providing them with given uniform ECD distribution in the testing zone.

The aim of the work is to create a method for nonlinear parametric surrogate synthesis of a movable frame of a non-axial homogeneous SECP with a planar ES structure. These systems provide uniform ECD distribution on the surface in the testing object area. A stochastic meta-heuristic algorithm for finding the global optimum for an extreme problem is implemented via the synthesis.

2. Formulation

2.1. Conceptual description of the optimal synthesis problem

Optimal ES synthesis procedures are applied to implement the initially given characteristics at the ECP design stage. This problem belongs to nonlinear inverse problems of mathematical modelling. As initial data for solving a nonlinear inverse problem, a given characteristic is used, providing a uniform distribution of the ECD $J_{reference}$ in the testing zone. A U-shaped form of the characteristic is applicable for the flaw problems when the ECD distribution is localized and maximally concentrated in the testing zone and outside it has a value close to zero. The synthesis problem task is formulated in the optimization formulation as a problem of quadratic functional minimizing. Taking into account certain peculiarities that are inherent in such a problem formulation in nonlinear mathematical programming, optimization methods have been chosen *i.e.*, modern metaheuristic stochastic optimization algorithms, both evolutionary and behavioural, are applied [12].

2.2. "Exact" model of the direct electrodynamic problem

First, let us address the direct electrodynamic problem solution for an EMF excitation source in the form of an infinitely thin rectangular loop, movable relative to the TO. A mathematical model of the interaction of such a field source with the TO is obtained by solving a boundary value problem in partial derivatives under the condition of tangential components continuity of the magnetic field strength and normal components of magnetic induction at the interfaces [13, 14]. The following assumptions were accepted – the TO medium was considered linear, isotropic and homogeneous. The investigated TO is of infinite size with thickness d with constant electrophysical parameters, namely, specific electrical conductivity σ and relative magnetic permeability μ_r . Above the TO at a height z_0 , there is an EMF source in the form of a coil with alternating current with intensity I and frequency ω , of a rectangular shape with dimensions $a \times b$. The EMF source moves in reference to the TO at a constant speed $\vec{v} = (v_x, v_y, 0)$.

As a result of solving Maxwell’s differential equations, the analytical dependences of the distribution of the complex magnetic induction components along the spatial coordinates B_x , B_y , B_z were obtained [13, 14]. Taking into account the previously introduced conventions:

$$k(d, \mu_r, \mu_0, \sigma, v_x, v_y, \omega) = \frac{1}{(1 - e^{2 \cdot \gamma \cdot d})}, \quad (1)$$

$$s(d, z, \mu_r, \mu_0, \sigma, v_x, v_y, \omega) = \left\{ -(1 + \lambda_0) \cdot e^{2 \cdot \gamma \cdot d} + v_0 \cdot e^{(\gamma - \sqrt{\xi^2 + \eta^2}) \cdot d} \right\} \cdot e^{\gamma \cdot z}, \quad (2)$$

$$c(d, z, \mu_r, \mu_0, \sigma, v_x, v_y, \omega) = \left\{ 1 + \lambda_0 - v_0 \cdot e^{(\gamma - \sqrt{\xi^2 + \eta^2}) \cdot d} \right\} \cdot e^{-\gamma \cdot z}, \quad (3)$$

the mathematical model for determining the ECD distribution components has the form:

$$J_x = \frac{1}{\mu_0 \cdot \mu_r} \cdot \left[\begin{array}{l} \frac{\partial}{\partial y} \left(j \cdot \frac{\mu_0 \cdot \mu_r \cdot I}{8 \cdot \pi^2} \cdot \int_{-\infty}^{\infty} \int_{-\infty}^{\infty} \frac{(\xi^2 + \eta^2) \cdot k(d, \mu_r, \mu_0, \sigma, v_x, v_y, \omega)}{\eta \cdot \gamma} \times \right. \\ \left. \times [s(d, z, \mu_r, \mu_0, \sigma, v_x, v_y, \omega) - c(d, z, \mu_r, \mu_0, \sigma, v_x, v_y, \omega)] \times \right. \\ \left. \times e^{-z_0 \cdot \sqrt{\xi^2 + \eta^2}} \cdot S(\xi, \eta) \cdot e^{-j(x \cdot \xi + y \cdot \eta)} d\xi d\eta \right) \\ \\ - \frac{\partial}{\partial z} \left(\frac{\mu_0 \cdot \mu_r \cdot I}{8 \cdot \pi^2} \cdot \int_{-\infty}^{\infty} \int_{-\infty}^{\infty} k(d, \mu_r, \mu_0, \sigma, v_x, v_y, \omega) \times \right. \\ \left. \times [s(d, z, \mu_r, \mu_0, \sigma, v_x, v_y, \omega) + c(d, z, \mu_r, \mu_0, \sigma, v_x, v_y, \omega)] \times \right. \\ \left. \times e^{-z_0 \cdot \sqrt{\xi^2 + \eta^2}} \cdot S(\xi, \eta) \cdot e^{-j(x \cdot \xi + y \cdot \eta)} d\xi d\eta \right) \end{array} \right], \quad (4)$$

$$J_y = \frac{1}{\mu_0 \cdot \mu_r} \cdot \left[\begin{array}{l} \frac{\partial}{\partial z} \left(\frac{\mu_0 \cdot \mu_r \cdot I}{8 \cdot \pi^2} \cdot \int_{-\infty}^{\infty} \int_{-\infty}^{\infty} \frac{\xi \cdot k(d, \mu_r, \mu_0, \sigma, v_x, v_y, \omega)}{\eta} \times \right. \\ \left. \times [s(d, z, \mu_r, \mu_0, \sigma, v_x, v_y, \omega) + c(d, z, \mu_r, \mu_0, \sigma, v_x, v_y, \omega)] \times \right. \\ \left. \times e^{-z_0 \cdot \sqrt{\xi^2 + \eta^2}} \cdot S(\xi, \eta) \cdot e^{-j(x \cdot \xi + y \cdot \eta)} d\xi d\eta \right) \\ \\ - \frac{\partial}{\partial x} \left(j \cdot \frac{\mu_0 \cdot \mu_r \cdot I}{8 \cdot \pi^2} \cdot \int_{-\infty}^{\infty} \int_{-\infty}^{\infty} \frac{(\xi^2 + \eta^2) \cdot k(d, \mu_r, \mu_0, \sigma, v_x, v_y, \omega)}{\eta \cdot \gamma} \times \right. \\ \left. \times [s(d, z, \mu_r, \mu_0, \sigma, v_x, v_y, \omega) - c(d, z, \mu_r, \mu_0, \sigma, v_x, v_y, \omega)] \times \right. \\ \left. \times e^{-z_0 \cdot \sqrt{\xi^2 + \eta^2}} \cdot S(\xi, \eta) \cdot e^{-j(x \cdot \xi + y \cdot \eta)} d\xi d\eta \right) \end{array} \right], \quad (5)$$

where $\mu_0 = 4 \cdot \pi \cdot 10^{-7}$ H/m (*i.e.* the magnetic constant in vacuum); $j = \sqrt{-1}$; $S(\xi, \eta)$ – function of a rectangular coil shape $S(\xi, \eta) = -j \cdot \frac{4}{\xi} \cdot \sin(a \cdot \xi) \cdot \sin(b \cdot \eta)$; ξ, η – variables of integration;

$$\gamma = \sqrt{\xi^2 + \eta^2 - j \cdot \sigma \cdot \mu_0 \cdot \mu_r \cdot (v_x \cdot \xi + v_y \cdot \eta) + j \cdot \omega \cdot \sigma \cdot \mu_0 \cdot \mu_r}, \quad (6)$$

$$\lambda_0 = \frac{\left\{ \gamma^2 - \mu_r^2 \cdot (\xi^2 + \eta^2) \right\} \cdot (1 - e^{-2 \cdot \gamma \cdot d})}{(\gamma + \mu_r \cdot \sqrt{\xi^2 + \eta^2})^2 - (\gamma - \mu_r \cdot \sqrt{\xi^2 + \eta^2})^2 \cdot e^{-2 \cdot \gamma \cdot d}}, \quad (7)$$

$$\nu_0 = \frac{4 \cdot \mu_r \cdot \gamma \cdot \sqrt{\xi^2 + \eta^2} \cdot e^{(\sqrt{\xi^2 + \eta^2} - \gamma) \cdot d}}{(\gamma + \mu_r \cdot \sqrt{\xi^2 + \eta^2})^2 - (\gamma - \mu_r \cdot \sqrt{\xi^2 + \eta^2})^2 \cdot e^{-2 \cdot \gamma \cdot d}}. \quad (8)$$

Let us consider an SECP with a rectangular planar ES structure which is a set of M ($i = 1, \dots, M$) sectional coils, each of which contains w_i turns. Their connection scheme is opposite or matched “across the field”. Such a rectangular planar ES structure is characterized by linear average dimensions of sides of each coil $a_{mi} \times b_{mi}$ and a rectangular section $q_i \times \tau_i$, whose dimensions are individual for each coil (Fig. 1). The location of all coils above the TO is determined by the average height z_m , *i.e.* the ES appears to be planar. At the same time excitation coils can be placed in space either uniformly or unevenly (Fig. 1).

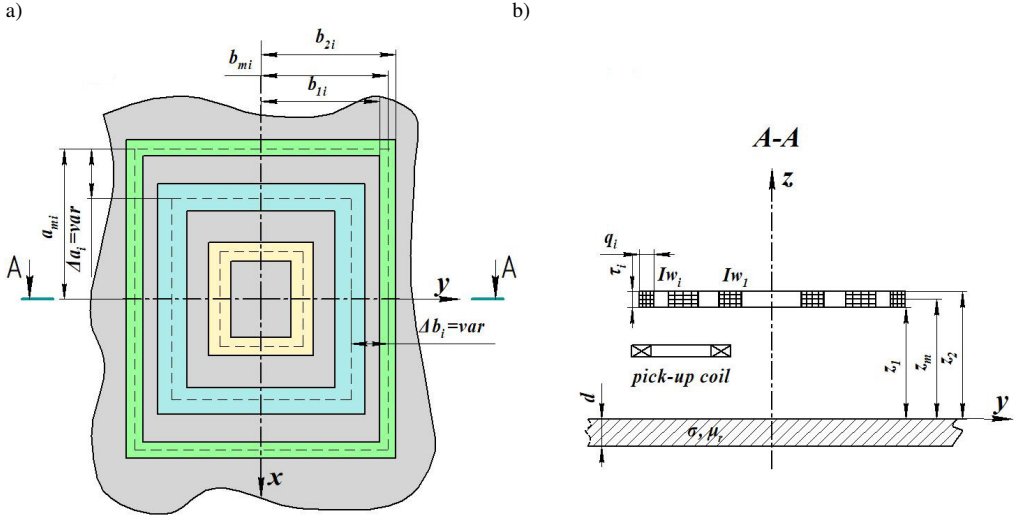


Fig. 1. Planar excitation system of a frame SECP: a) general view; b) section A-A.

An analytical mathematical model of a rectangular coil ES SECP is obtained on the basis of the mathematical model of a thin rectangular loop (4), (5), by additional integration over the cross-sectional area at a constant current density in it. In particular, in expressions (4) and (5), the component $S(\xi, \eta) \cdot e^{-z_0 \cdot \sqrt{\xi^2 + \eta^2}}$ is replaced by the relations obtained by integrating over the cross-sectional area [14]:

$$\begin{aligned} \frac{w}{q \cdot \tau} \cdot \left[\int_{-q/2}^{q/2} \sin((a_m + p) \cdot \xi) \cdot \sin((b_m + p) \cdot \eta) dp \right] \cdot \left[\int_{z_m - \tau/2}^{z_m + \tau/2} e^{-g \cdot \sqrt{\xi^2 + \eta^2}} dg \right] = \\ = \frac{w}{q \cdot \tau} \cdot I_s(a_m, b_m, q) \cdot I_E(z_m, \tau), \quad (9) \end{aligned}$$

where $q = b_2 - b_1$; $\tau = z_2 - z_1$; $z_m = (z_1 + z_2)/2$; $b_m = (b_1 + b_2)/2$; $z_m = (z_1 + z_2)/2$ the average value of the dimensions and height of the coil are above the TO, respectively; p, g – variables of integration.

The analytical expression for the component $I_E(z_m, \tau)$ is as follows:

$$I_E(z_m, \tau) = \int_{z_m - \tau/2}^{z_m + \tau/2} e^{-g \cdot \sqrt{\xi^2 + \eta^2}} dg = \frac{e^{z_m \cdot \sqrt{\xi^2 + \eta^2}}}{\sqrt{\xi^2 + \eta^2}} \cdot \left(e^{-\left(\frac{\tau}{2} \cdot \sqrt{\xi^2 + \eta^2}\right)} - e^{\left(\frac{\tau}{2} \cdot \sqrt{\xi^2 + \eta^2}\right)} \right). \quad (10)$$

The final mathematical model of the ES SECP coil which determines the distribution of ECD on the surface of the TO, taking into account the above relations, has the following form:

$$J_x = \frac{1}{\mu_0 \cdot \mu_r} \cdot \left[\begin{array}{l} \frac{\partial}{\partial y} \left(\frac{\mu_0 \cdot \mu_r \cdot I \cdot w}{2 \cdot \pi^2 \cdot q \cdot \tau} \cdot \int_{-\infty}^{\infty} \int_{-\infty}^{\infty} \frac{(\xi^2 + \eta^2) \cdot k(d, \mu_r, \mu_0, \sigma, v_x, v_y, \omega)}{\xi \cdot \eta \cdot \gamma} \times \right. \\ \left. \times [s(d, z, \mu_r, \mu_0, \sigma, v_x, v_y, \omega) - c(d, z, \mu_r, \mu_0, \sigma, v_x, v_y, \omega)] \times \right. \\ \left. \times e^{-j(x \cdot \xi + y \cdot \eta)} \cdot I_s(a_m, b_m, q) \cdot I_E(z_m, \tau) d\xi d\eta \right) - \\ \frac{\partial}{\partial z} \left(-j \frac{\mu_0 \cdot \mu_r \cdot I \cdot w}{2 \cdot \pi^2 \cdot q \cdot \tau} \cdot \int_{-\infty}^{\infty} \int_{-\infty}^{\infty} \frac{k(d, \mu_r, \mu_0, \sigma, v_x, v_y, \omega)}{\xi} \times \right. \\ \left. \times [s(d, z, \mu_r, \mu_0, \sigma, v_x, v_y, \omega) + c(d, z, \mu_r, \mu_0, \sigma, v_x, v_y, \omega)] \times \right. \\ \left. \times e^{-j(x \cdot \xi + y \cdot \eta)} \cdot I_s(a_m, b_m, q) \cdot I_E(z_m, \tau) d\xi d\eta \right) \end{array} \right], \quad (11)$$

$$J_y = \frac{1}{\mu_0 \cdot \mu_r} \cdot \left[\begin{array}{l} \frac{\partial}{\partial z} \left(-j \frac{\mu_0 \cdot \mu_r \cdot I \cdot w}{2 \cdot \pi^2 \cdot q \cdot \tau} \cdot \int_{-\infty}^{\infty} \int_{-\infty}^{\infty} \frac{k(d, \mu_r, \mu_0, \sigma, v_x, v_y, \omega)}{\eta} \times \right. \\ \left. \times [s(d, z, \mu_r, \mu_0, \sigma, v_x, v_y, \omega) + c(d, z, \mu_r, \mu_0, \sigma, v_x, v_y, \omega)] \times \right. \\ \left. \times e^{-j(x \cdot \xi + y \cdot \eta)} \cdot I_s(a_m, b_m, q) \cdot I_E(z_m, \tau) d\xi d\eta \right) - \\ \frac{\partial}{\partial x} \left(\frac{\mu_0 \cdot \mu_r \cdot I \cdot w}{2 \cdot \pi^2 \cdot q \cdot \tau} \cdot \int_{-\infty}^{\infty} \int_{-\infty}^{\infty} \frac{(\xi^2 + \eta^2) \cdot k(d, \mu_r, \mu_0, \sigma, v_x, v_y, \omega)}{\xi \cdot \eta \cdot \gamma} \times \right. \\ \left. \times [s(d, z, \mu_r, \mu_0, \sigma, v_x, v_y, \omega) - c(d, z, \mu_r, \mu_0, \sigma, v_x, v_y, \omega)] \times \right. \\ \left. \times e^{-j(x \cdot \xi + y \cdot \eta)} \cdot I_s(a_m, b_m, q) \cdot I_E(z_m, \tau) d\xi d\eta \right) \end{array} \right]. \quad (12)$$

The mathematical model of a real ES for calculating the ECD distribution is very complicated since it contains both improper multiple integrals of the first kind and integration over the cross-sectional area of the coils. The computational time resource intensity of the model is quite large. It is clear that the use of a complex and resource-intensive mathematical model for optimal synthesis significantly complicates the solution. The use of surrogate optimization technology provides for the replacing the resource-intensive electrodynamic model with its approximated analogue – a metamodel. This, in turn, allows to avoid cumbersome calculations and is widely used by scientists in various fields of research [15–18]. The authors have successfully used this approach in optimal synthesis of circular a non-axial SECP with planar and volumetric ES structures which is discussed in [19–21]. A detailed algorithm for performing

surrogate SECP optimization, consisting in the step-by-step execution of a number of tasks using modern achievements of artificial intelligence technologies and the theory of experiment planning for both simple and more complex cases of approximation of response hypersurfaces, is described in [19–21]. Therefore, in this case, before addressing the problem of optimal synthesis, it is necessary first to design a movable SECP metamodel with a rectangular planar ES structure.

2.3. Computer design of the experiment. Metamodel design

The functional approximation dependence of ECD distribution for a movable SECP is multi-dimensional $\hat{J} = f(x, y, a, b)$ and depends on several parameters, namely, the spatial coordinates x and y on the TO surface in the testing zone and the geometric dimensions a and b of the ES coil sections. For the design of a multivariate approximation model, RBF-neural networks, that is, *neural networks* (NN) based on radial-basis functions, have proven themselves well due to their universal approximation properties. As shown in [11, 19–21], on their basis and using a hybrid approach with various methods of increasing the accuracy, it is possible to obtain metamodels with acceptable approximation error. Therefore, the authors opted for them with the simultaneous implementation of the decomposition of the search area into several subdomains, with the application of the additive NN-regression and network committees at each of its levels.

To design a multidimensional metamodel, an array of the training sample was created by calculating the ECD distribution with functional dependencies (11), (12) in the general case. Computer methods to uniformly fill the search hyperspace with reference points, that is the optimal *designs of computational experiments* (DOEs) [22], were used to form such an array. The use of DOEs with topology uncertainty of the hypersurface increases the probability of the reference points falling into the areas of extremes and kinds. [23] shows that the best characteristics of the homogeneity of a multidimensional DOE can be achieved on the basis of quasi-random parameterless additive recursive R-sequences and combinations of Sobol's LP_7 -sequences.

Let us give a model example of creating a metamodel of a frame movable SECP with a planar ES structure with the following initial dates: $d = 10$ mm, $z_0 = 3$ mm, $I = 1$ A, $f = 1$ kHz, $\sigma = 3.74510^7$ S/m, $\mu_r = 1$, $\vec{v} = (40, 0, 0)$ m/s. The parameters of the varying model were set in the range: $x = -35, \dots, 35$ mm; $y = 0, \dots, 25$ mm. Square ES turns $a = 3, \dots, 15$ mm are considered.

To design a multidimensional metamodel, the search space is decomposed into six subdomains along the linear dimensions of the square loop. A data array with the number of points $N_{training}$ to train additive NN-regression was formed for each of the obtained subdomains using DOE based via R_3 -sequences. At the same time, for each subdomain, the number of DOE points is set individually. The formation of subsamples for training, testing and reconstruction control is carried out via the bagging procedure.

To obtain the acceptable accuracy at the training stage, additive NN-regression is applied. The number of its intermediate levels is determined by the value of the relative average error of the *MAPE* approximation, not exceeding 15%. At each intermediate level of NN-regression, network committees are used, the productivity of which is more than 90%, and decision-making is applied by averaging over the ensemble. Due to this hybrid design of additive NN-regression, it was possible to obtain the *MAPE* value for the complex topology of the ECD distribution at the level from 7.38% to 14.91% at the stage of training.

As an example, Table 1 provides information on the design of a metamodel for one subdomain $7 \leq a \leq 9$ mm. First, four intermediate levels of $\hat{J}_1 - \hat{J}_4$ additive NN-regression are shown. For each of them, a set of NN is given, selected for the formation of the committee. Second, the same table for each intermediate level of additive NN-regression presents the obtained numerical value of *MAPE*, the mean square of the residual *MS_R* and the standard error of assessing the adequacy of *S_R*. In addition to the statistical indicators shown in Table 1, the metamodels created are assessed according to a number of other qualitative and quantitative indicators [24].

Table 1. Information on metamodel creation of a square movable SECP with a planar ES structure for a slices of $7 \leq a \leq 9$ mm ($N_{training} = 2076$) at the stages of TS training and RS reconstitution of the response surface.

ANN – regression level	Neural networks constituting committees	MAPE, %		MS _R		S _R	
		TS	RS	TS	RS	TS	RS
\hat{J}_1	RBF-3-330-1(32)	11.53	12.14	0.00299	0.00285	0.0547	0.053
	RBF-3-297-1(83)						
	RBF-3-245-1(386)						
	RBF-3-306-1(200)						
	RBF-3-283-1(291)						
\hat{J}_2	RBF-3-200-1(6)	9.02	9.42	0.00224	0.00228	0.0473	0.0478
	RBF-3-240-1(57)						
	RBF-3-302-1(129)						
	RBF-3-304-1(142)						
	RBF-3-304-1(144)						
\hat{J}_3	RBF-3-300-1(116)	7.96	8.54	0.00187	0.00203	0.0432	0.045
	RBF-3-297-1(96)						
	RBF-3-274-1(69)						
	RBF-3-281-1(74)						
	RBF-3-300-1(113)						
\hat{J}_4	RBF-3-195-1(2)	7.38	7.97	0.00174	0.00193	0.0416	0.0439
	RBF-3-273-1(11)						
	RBF-3-297-1(36)						

3. Verification of the created metamodel

The following obligatory step is to check the resulting metamodel. The response hypersurface was reproduced in all subregions at a number of points $N_{reconstitution} = 4090$ for this kind of the examination. And the aggregate of statistical indicators assessed its adequacy and information content [24]. Some of these indicators are shown in Table 1. For other subregions, the *MAPE* error at the stage of reproduction ranged from 7.97% to 14.24%. The reproduction of the response surface using the obtained metamodel is performed over the entire range of variation of the variables at a much larger number of points than at the training stage ($N_{reconstitution} > N_{training}$). The results of reconstitution in the form of level lines for some surface slices are shown in Fig. 2.

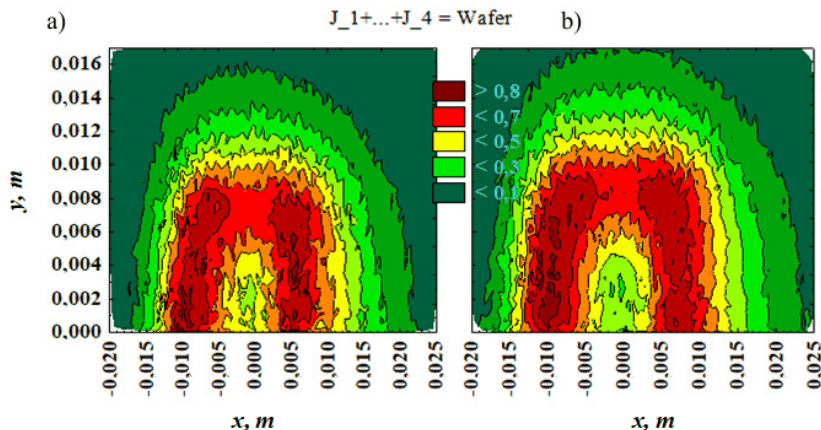


Fig. 2. Reconstitution of the response surface ($7 \leq a \leq 9$ mm) using the metamodel for a moving square SECP with a planar ES structure: a) level lines for slicing surface $7 \leq a \leq 8$ mm; b) level lines for slicing surface $8 \leq a \leq 9$ mm.

Also, for a qualitative assessment of the reconstitution of the response hypersurface and better visual perception of the simulation results, graphic material is presented in the form of scatter diagrams (Fig. 3) and histograms of the distribution of *MAPE* relative errors (Fig. 4).

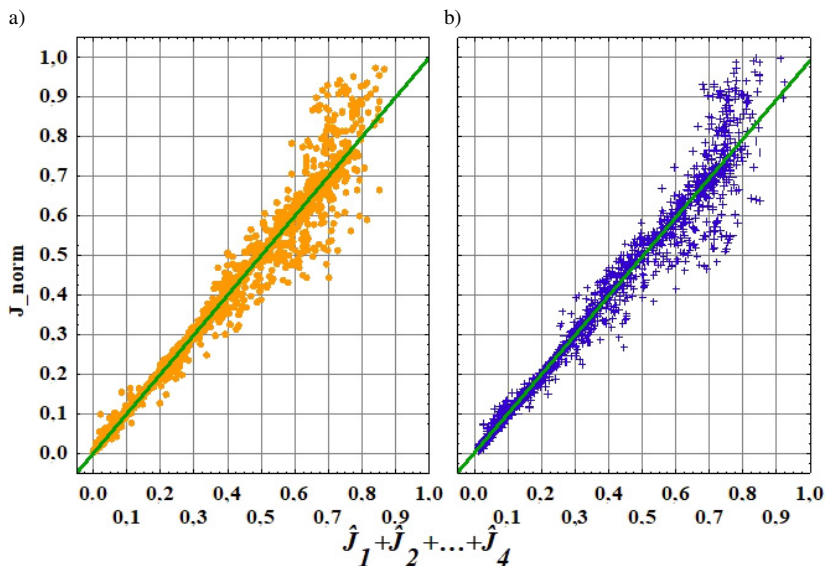


Fig. 3. Scatter diagrams of the values of the multidimensional metamodel for the subdomain $7 \leq a \leq 9$ mm at the stage of reconstitution: a) slice $7 \leq a \leq 8$ mm; b) slice $8 \leq a \leq 9$ mm.

At the same time, the quality of the obtained metamodel is additionally checked by reconstruction of the response hypersurface according to the formula describing the output of the additive NN-regression dependence based on RBF-neural networks. So in Fig. 5, for example, reconstitutions of the response hypersurface are shown for slices $a = 8.5$ mm, $a = 10.5$ mm, $a = 14.5$ mm at a height above the TO $z_0 = 3$ mm.

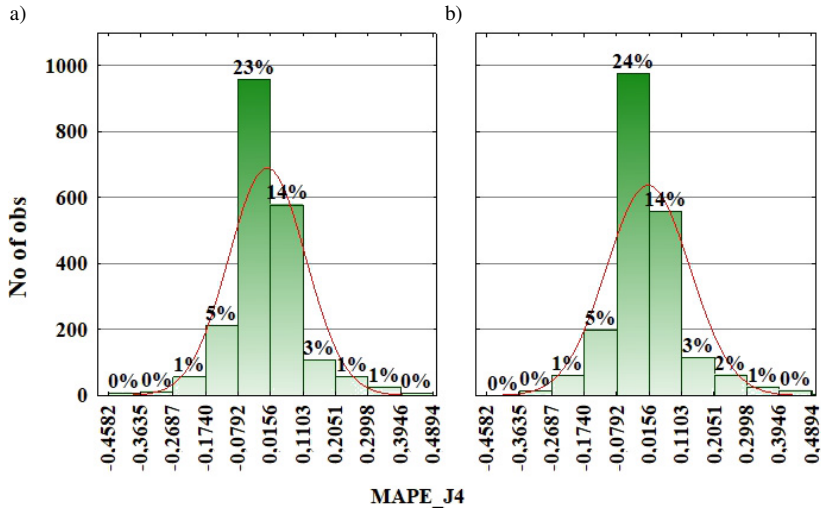


Fig. 4. Histograms of distribution of the relative model error of approximation of the response hypersurface: a) slice $7 \leq a \leq 8$ mm; b) slice $7 \leq a \leq 9$ mm.

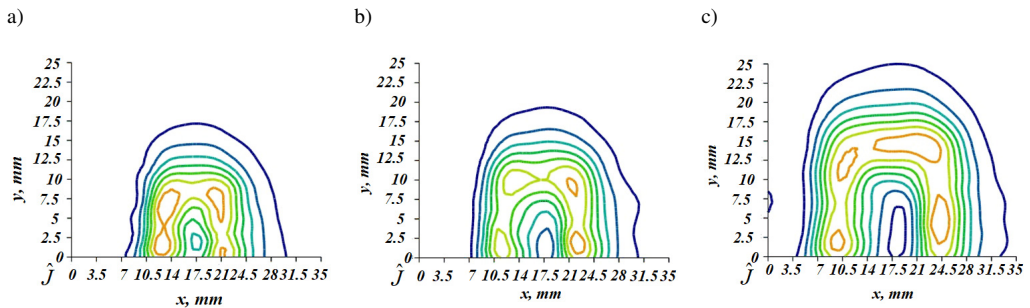


Fig. 5. Reconstruction of the response surface using an approximation model for a movable square SECP with a planar ES structure at a height of $z_0 = 3$ mm: a) level lines for surface slice $a = 8.5$ mm; b) level lines for surface slice $a = 10.5$ mm; c) level lines for the surface slice $a = 14.5$ mm.

4. Optimal ES synthesis

Using the created additive NN-metamodel, we present a solution to the problem of optimal synthesis nonlinear a surrogate of an SECP with the uniform sensitivity in the testing zone. We will use stochastic optimization methods, which have given a good account of themselves when searching for global extrema [12, 25]. It should be noted that of all the applied evolutionary and behavioural algorithms, the best results are obtained using hybrid algorithms, namely, these created on the basis of a genetic algorithm with a local search with the Nelder-Mead simplex method and a population metaheuristic optimization algorithm by a swarm of particles with evolutionary formation of the swarm composition. The latter is a low-level hybridization of the genetic algorithm and the PSO algorithm [12].

Variants of ES structures with different numbers of square sectional turns $M = 3-5$ were specified for the numerical modelling. As a result of solving the nonlinear inverse problem, the

magnetomotive forces Iw_i and the geometric dimensions of sectional turns a_i are determined. The obtained numerical results are presented in Table 2. Together, these parameters ensure the approximation of the created ECD distribution (Fig. 6d, e, f graph 2) to the initially given U-shaped (Fig. 6d, e, f graph 1) on the surface of the TO in the testing zone.

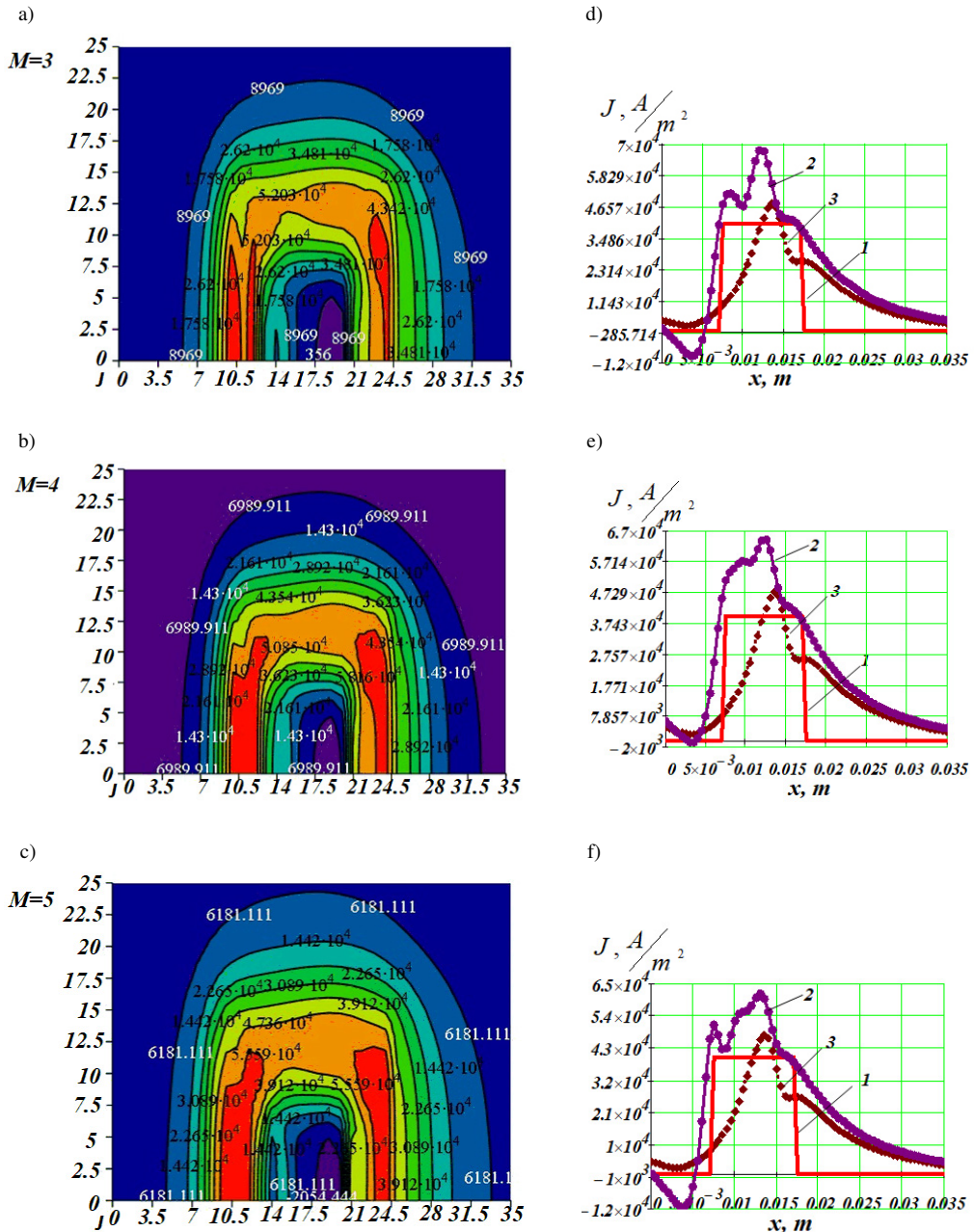


Fig. 6. Results of the synthesis of movable SECP with a square planar ES, calculated in accordance with the “exact” electrodynamic model: (a), (b), (c) lines of the ECD distribution level; (d), (e), (f) the ECD distribution along the Ox axis.

Table 2. The results of nonlinear surrogate synthesis of a square movable SECP with the variants of the ES structure.

Synthesized excitation systems	$M = 3$		$M = 4$		$M = 5$	
	a , mm	Iw , A × turns	a , mm	Iw , A × turns	a , mm	Iw , A × turns
No.	a , mm	Iw , A × turns	a , mm	Iw , A × turns	a , mm	Iw , A × turns
1	6.39	-0.837	6.37	-0.649	6.64	-1.495
2	9.5	1.1	8.183	0.398	7.98	1.246
3	13.5	1.15	10.23	0.9324	10.96	0.613
4	–	–	13.49	0.92	11.15	0.205
5	–	–	–	–	14.26	0.82

The numerical synthesis results with the initially given U-shaped ECD distribution in the testing zone $7 \leq x, y \leq 17$ mm for three variants of SECPs with planar ES structures and the number of sectional turns $M = 3, 4, 5$ are shown in Fig. 6. Table 2 schematically presents the designs of the synthesized ES probes. ECD distributions J (A/m²) are given in the form of level lines which are created by synthesized ES (Fig. 6a, b, c) and calculated in accordance with the “exact” electrodynamic model.

To visually compare the synthesized and initially given ECD distributions, graphs of their changes along the Ox axis where presented. Also, the same figures showed the ECD distribution created with a single square turn measuring 15×15 mm (Fig. 6d, e, f, graph 3). Therefore, for the synthesized ES structures, a comparative analysis of the ECD distributions obtained showed almost the same excess of the EC intensity level for all variants, which differ in the fulfilment of the uniformity conditions. One should consider the excess of the EC intensity level over the given one to be very promising as it potentially offers better conditions for detecting defects. The best result in terms of homogeneity are given by an ES with four sectional turns. It should be also noted that the simpler and more complex than the given structure of the ES did not allow for achieving a better result. All the variants of the structures under consideration showed the best results in terms of homogeneity of ECD distribution in comparison with the classical SECP with an ES when they were in the form of a single square turn.

5. Conclusions

The authors have proposed a novel method of surrogate nonlinear parametric synthesis of a movable SECP with a rectangular planar ES structure. The synthesis provides a close to uniform ECD distribution on the surface in the testing object zone and allows for the same sensitivity to defects. To implement the method, algorithms and software have been developed for calculating

the direct problem using an “exact” electrodynamic model and implementing a multidimensional effective DOE based on R-sequences with low rates of centered and wrap-around discrepancies. A technique for improving the approximation capabilities of NN-regression models has been developed which enables simultaneous use of additive NN-regression technologies with associative machine techniques and search area decomposition. Due to complexity of structural features of additive NN-regression, *i.e.* the use of NN committees at each intermediate level of approximation, it became possible to achieve an acceptable *MAPE* error of the multidimensional SECP metamodel. This contributed to the successful solution of the formulated synthesis problem. Algorithms for conditional surrogate SECP optimization have been developed on the basis of modern population metaheuristic stochastic hybrid algorithms for finding global extrema. Numerous experiments have illustrated the efficiency of solving the problem of nonlinear surrogate synthesis of a square movable SECP with a planar ES structure. Its advantage over the classical analogue has been proved.

References

- [1] Rosado, L. S., Gonzalez, J. C., Santos, T. G., Ramos, P. M., & Piedad, M. (2013). Geometric optimization of a differential planar eddy currents probe for non-destructive testing. *Sensors and Actuators A: Physical*, 197, 96–105. <https://doi.org/10.1016/j.sna.2013.04.010>
- [2] Su, Z., Efremov, A., Safdarnejad, M., Tamburrino, A., Udpa, L., & Udpa, S. (2015). Optimization of coil design for near uniform interrogating field generation. *AIP Conference Proceedings*, 1650, 405–413. <https://doi.org/10.1063/1.4914636>
- [3] Su, Z., Ye, C., Tamburrino, A., Udpa, L., & Udpa, S. (2016). Optimization of coil design for eddy current testing of multi-layer structures. *International Journal of Applied Electromagnetics and Mechanics*, 52(1–2), 315–322. <https://doi.org/10.3233/JAE-162030>
- [4] Liu, Z., Yao, J., He, C., Li, Z., Liu, X., & Wu, B. (2018). Development of a bidirectional-excitation eddy-current sensor with magnetic shielding: Detection of subsurface defects in stainless steel. *IEEE Sensors J.*, 18(15), 6203–6216. <https://doi.org/10.1109/JSEN.2018.2844957>
- [5] Ye, C., Udpa, L., & Udpa, S. (2016). Optimization and Validation of Rotating Current Excitation with GMR Array Sensors for Riveted Structures Inspection. *Sensors*, 16(9), 1512. <https://doi.org/10.3390/s16091512>
- [6] Rekanos, I. T., Antonopoulos, C. S., & Tsiboukis, T. D. (1999). Shape design of cylindrical probe coils for the induction of specified eddy current distributions. *IEEE Transactions Magnetics*, 35(3), 1797–1800. <https://doi.org/10.1109/20.767380>
- [7] Li, Y., Ren, S., Yan, B., Zainal Abidin, I. M., & Wang, Y. (2017). Imaging of subsurface corrosion using gradient-field pulsed eddy current probes with uniform field excitation. *Sensors*, 17, 1747. <https://doi.org/10.3390/s17081747>
- [8] Hashimoto, M., Kosaka, D., Ooshima, K., & Nagata, Y. (2002). Numerical analysis of eddy current testing for tubes using uniform eddy current distribution. *International Journal of Applied Electromagnetics and Mechanics*, 15(1–4), 27–32. <https://doi.org/10.3233/JAE-2002-511>
- [9] Repelianto, A. S., Kasai, N., Sekino, K., & Matsunaga, M. (2019). A Uniform Eddy Current Probe with a Double-Excitation Coil for Flaw Detection on Aluminium Plates. *Metals*, 9(10), 1116. <https://doi.org/10.3390/met9101116>
- [10] Halchenko, V. Ya., Trembovetskaya, R. V., & Tychkov, V. V. (2020). Surface eddy current probes: excitation systems of the optimal electromagnetic field (review). *Devices and Methods of Measurements*, 11(2), 91–104. <https://doi.org/10.21122/2220-9506-2020-11-2-91-104>

- [11] Trembovetska, R. V., Halchenko, V. Ya., Tychkov, V. V., & Storchak, A. V. (2020). Linear Synthesis of Uniform Anaxial Eddy Current Probes with a Volumetric Structure of the Excitation System. *International Journal “NDT Days”*, 3(4), 184–190. <https://www.bg-s-ndt.org/journal/vol3/JNDTD-v3-n4-a01.pdf> (in Russian)
- [12] Halchenko, V. Ya., Yakimov, A. N., & Ostapuschenko, D. L. (2010). Global optimum search of functions with using of multiagent swarm optimization hybrid with evolutionary composition formation of population. *Information Technology*, 10, 9–16. <http://novtex.ru/IT/it2010/It1010.pdf> (in Russian)
- [13] Itaya, T., Ishida, K., Kubota, Y., Tanaka, A., & Takehira, N. (2016). Visualization of Eddy Current Distributions for Arbitrarily Shaped Coils Parallel to a Moving Conductor Slab. *Progress In Electromagnetics Research M*, 47, 1–12. <https://doi.org/10.2528/PIERM16011204>
- [14] Itaya, T., Ishida, K., Tanaka, A., Takehira, N., & Miki, T. (2012). Eddy Current Distribution for a Rectangular Coil Arranged Parallel to a Moving Conductor Slab. *IET Science, Measurement & Technology*, 6(2), 43–51. <https://doi.org/10.1049/iet-smt.2011.0015>
- [15] Koziel, S., & Bekasiewicz, A. (2017). *Multi-objective design of antennas using surrogate models*. World Scientific Publishing Europe Ltd.
- [16] Forrester, A. I. J., Sóbester, A., & Keane, A. J. (2008). *Engineering design via surrogate modelling: a practical guide*. Chichester: Wiley.
- [17] Burnaev, E. V., Erofeev, P., Zaitsev, A., Kononenko, D., & Kapushev E. (2015). *Surrogate modeling and optimization of the airplane wing profile based on Gaussian processes*. <http://itas2012.iitp.ru/pdf/1569602325.pdf> (in Russian)
- [18] Koziel, S., Echeverría Ciaurri, D., & Leifsson L. (2011). Surrogate-based methods. In Koziel S., Yang X.S. (Eds.), *Computational Optimization, Methods and Algorithms. Studies in Computational Intelligence*, 356, Springer-Verlag. https://doi.org/10.1007/978-3-642-20859-1_3
- [19] Halchenko, V. Ya., Trembovetska, R. V., Tychkov, V. V., & Storchak, A. V. (2019). Nonlinear surrogate synthesis of the surface circular eddy current probes. *Przegląd Elektrotechniczny*, 9, 76–82. <https://doi.org/10.15199/48.2019.09.15>
- [20] Halchenko, V. Ya., Trembovetska, R. V., & Tychkov, V. V. (2019). Linear synthesis of non-axial surface eddy current probes. *International Journal “NDT Days”*, 2(3), 259–268. <https://www.ndt.net/article/NDTDays2019/papers/JNDTD-v2-n3-a03.pdf> (in Russian)
- [21] Trembovetska, R. V., Halchenko, V. Y., & Tychkov, V. V. (2019). Multiparameter hybrid neural network metamodel of eddy current probes with volumetric structure of excitation system. *International Scientific Journal Mathematical Modeling*, 4(3), 113–116. <https://stumejournals.com/journals/mm/2019/4/113>
- [22] Koshevoy, N. D., Gordienko, V. A., & Sukhobrus, Ye. A. (2014). Optimization for the design matrix realization value with the aim to investigate technological processes. *Telecommunications and radio engineering*, 73(15), 1383–1386. <https://doi.org/10.1615/TelecomRadEng.V73.i15.60> (in Russian)
- [23] Halchenko, V. Ya., Trembovetska, R. V., Tychkov, V. V., & Storchak, A. V. (2020). The Construction of Effective Multidimensional Computer Designs of Experiments Based on a Quasi-random Additive Recursive Rd–sequence. *Applied Computer Systems*, 25(1), 70–76. <https://doi.org/10.2478/acss-2020-0009>
- [24] Brink, H., Richards, J., & Fetherolf, M. (2017). *Real-World Machine Learning*. Manning Publications Co.
- [25] Kuznetsov, B. I., Nikitina, T. B., & Bovdii, I. V. (2020). Active shielding of magnetic field of overhead power line with phase conductors of triangle arrangement. *Tekhnichna elektrodynamika*, 4, 25–28. <https://doi.org/10.15407/techned2020.04.025>



Volodymyr Ya. Halchenko received the Doctor Tech. Sc. degree from Kharkiv State Polytechnic University, Ukraine, in 1999. He is currently Full Professor at the Department of Instrumentation, Mechatronics and Computer Technologies of Cherkasy State Technological University. He has authored or coauthored over 320 publications. He is a member of the Ukrainian Society for Non-Destructive Testing. His current research interests include non-destructive testing, mathematical modelling, optimization and intellectual data analysis.

emational modelling, optimization and intellectual data analysis.



Volodymyr Tychkov received the Cand. Tech. Sc. degree from Cherkasy State Technological University, Ukraine in 2017. He is Associate Professor at the Department of Instrumentation, Mechatronics and Computer Technologies of Cherkasy State Technological University. He has authored or coauthored over 240 publications. He is a member of the Ukrainian Society for Non-Destructive Testing and the Ukrainian Academy of Engineering Sciences. His current research interests include non-destructive testing, mathematical modelling, optimization and intellectual data analysis.

ests include non-destructive testing, mathematical modelling, optimization and intellectual data analysis.



Ruslana Trembovetska received the Cand. Tech. Sc. degree from Cherkasy State Technological University, Ukraine in 2005. She is Associate Professor at the Department of Instrumentation, Mechatronics and Computer Technologies of Cherkasy State Technological University. She has authored or coauthored over 335 publications. She is currently a member of the Ukrainian Society for Non-Destructive Testing. Her current research interests include non-destructive testing, mathematical modelling, optimization and intellectual data analysis.

destructive testing, mathematical modelling, optimization and intellectual data analysis.